C.   PROJECT DESCRIPTION

1. RESULTS FROM PRIOR SUPPORT

This is my first proposal to NSF as a PI.

2. SIGNIFICANCE OF THE PROPOSED PROJECT AND PREVIOUS WORK

In 1967, Aki [1967] proposed that the earthquake rupture process is scale invariant. Since then, a number of investigators have contributed observations of stress drop and apparent stress across a large range of moments [Gibowicz et al, 1991, Abercrombie, 1995b, Nadeau and Johnson, 1998, Johnson and Nadeau, 2002, McGarr, 1999, Jost et al, 1998, Mayeda and Walter, 1996, Perez-Campos and Beroza, 2001, Prejean and Ellsworth, 2001, Ide and Beroza, 2001, Ide et al 2003]. While some of the papers appear to confirm Aki's conjecture, others suggest that it may not hold, and the controversy continues. Perhaps one of the best compilations of results is Figure 3 of Ide and Beroza [2001]. The authors collected observations of the ratio of radiated energy to seismic moment spanning 19 decades of moment and concluded that scaling invariance holds. They show that in many individual studies, the decrease in stress during an event appears to increase with increasing event moment. In contrast, the results from various experiments across the large range of moments from microfractures in laboratory experiments to great earthquakes are consistent with the stress change being, on average, independent of moment. They explain apparent discrepancies observed for small events as high frequency seismic energy missing due to attenuation along the path or to the finite bandwidth of the recording instrument. In their Figure 3, Ide and Beroza [2001] show two gray triangles in the moment range between 10^{10} Nm and 10^{15} Nm, where scaling still appears to breakdown. They suggest that in this range, corresponding to magnitudes between 0.5 and 4, some events may be "missing". The low end of this magnitude range, around 1.5 or 2, is the point at which catalogs generally become incomplete, and there are few cases in which earthquakes or fractures have occured at such a small distances from a station that even the smallest shocks are recorded well enough to study the physics of the rupture process. Other questions about the physics of tiny earthquakes also remain open, because of the dearth of high-quality observations. How small can aftershocks be, and are they statistically [for a review see Shcherbakov et al, 2005] and physically [Das and Henry, 2003], related to their mainshock in the same way as larger earthquakes? Do tiny earthquakes exhibit complexity? What are the effects of attenuation [Abercrombie, 1997, 1998, 2000] and/or f_{max} [Hanks, 1982] on the frequency content of the recordings and thus the interpretation of the source?

Sequences of small earthquakes near Berkeley Seismological Laboratory's (BSL) station BRIB (37.92 N, 122.15 W, Figure 1) provide an opportunity to explore such questions. At the surface this station has a Guralp CMG-3T and a FBA-23 accelerometer, with data recorded continuously at 80 sps, 20/40 sps and at slower rate. In addition, a 3-component Oyo HS-1 geophone and a 3-component Wilcoxon 731A accelerometer sampled at 500 sps are emplaced in a borehole at a depth of 119 m, and a Sacks-Evertson Dilational Strainmeter at 162 m. Since the beginning of October 2003, the vertical component of the geophone has been recorded continuously at 500 sps, while the two horizontal geophone components and the single functioning

horizontal component of the accelerometer are recorded as triggered data at 500 sps. This station is an element of the Berkeley Digital Seismic Network (BDSN) and of the Northern Hayward Fault Network (NHFN), which together with the Northern California Seismic Network (NCSN) monitor seismicity in the San Francisco Bay Area.

On 19 Oct 2003 at 14:35:27 UTC, a M_d 2.5 earthquake (FS, Figure 2A) occurred almost directly below BRIB. It was followed just under one hour later by a M_L 3.5 mainshock (MS, Figure 2B) and more than 4000 aftershocks ranging in magnitude (Figure 3) over the course of the next 3 months. Both the MS and a major aftershock (MAS, Figure 2C) the following day with M_L 3.4 caused steps on the strainmeter record. Over the course of the past 2 years, we have looked at the borehole recordings of a small subset of the events, about 100
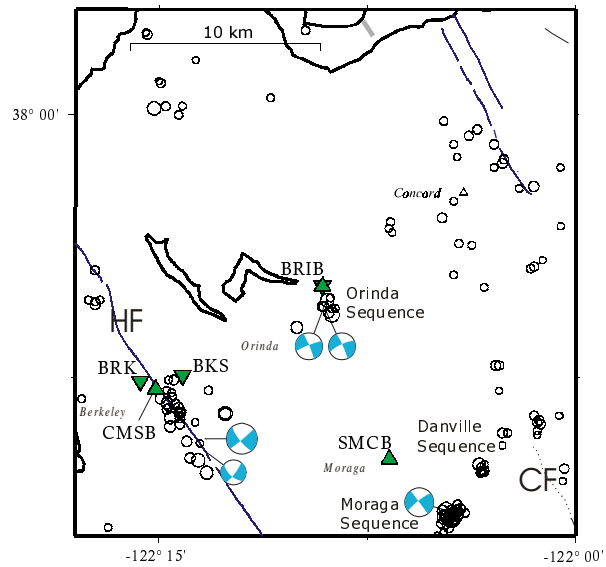

Figure 1: Map showing locations of BDSN stations (inverted triangles) and NHFN stations (triangles), as well as the events from the Orinda and Moraga earthquake sequences. The moment tensors are taken from the Berkeley Regional Moment Tensor catalog, event locations are taken from the NCSN catalog. Traces of the Hayward (HF) and Calveras (CF) Faults are also shown.

[Hellweg, 2004, 2005a, 2005b, 2006]. For the recordings at BRIB, the differences in path are small. The MS is small, so the aftershocks populate a very small volume. As an indication, t_{S-P} lies between 0.58 s and 0.72 s, so the hypocentral distances from the station are less than 5 km and differ by a little less than 1 km, assuming standard wave velocities in the region. The waveforms recorded on the borehole instrument for the large events of the sequence, as well as the very small events are very simple (Figures 2, 5), despite the fact that the borehole is shallow compared to others (Jost et al, 1998, Abercrombie, 1995b, Ide et al, 2003). Most of the Orinda events are so small, they were recorded only at BRIB; the NCSN catalog lists about 15 of the largest. Using these catalog magnitudes and Richter's [1935] procedure for determining M_L, I calibrated a "manual magnitude" scale (Figure 4) [Hellweg 2004, 2006], and determined that for the smallest events $M_L \sim$ –2.5. The range $M_L \sim$ –2.5 – 3.5 corresponds to moments from 10^5 to 10^{14} Nm, the range with Ide and Beroza's (2001) missing events. Since 2003, other sequences have occurred nearby, producing further clusters of low magnitude seismicity.

We will explore the scaling of moment, energy and stressdrop over the entire range of event sizes first for the Orinda sequence and later for the other nearby sequences, using measurements from P- as well as S-waves, in both the time [Seidl and Hellweg, 1988] and frequency [Abercrombie, 1995b] domains. To calculate the stressdrop it is necessary to know the moment and a source dimension. For small events, these are usually calculated from the low frequency level of the spectrum and its corner frequency, respectively. However, when the seismogram is relatively simple, as it is for the events of the Orinda sequence recorded on the borehole sensors

at BRIB (Figures 2, 5), the moment and source dimension can also be calculated from time domain measurements of the integral under the displacement pulse and its duration [Seidl and Hellweg, 1988]. It will be interesting to compare estimates of stress drop and apparent stress for events of different sizes using both time and frequency domain measurements, as initial measurements of the P- and S- pulses have shown that for small events, the P-pulse continues to decrease in duration with decreasing magnitude, while the S-pulse appears to stagnate at about 0.1 s [Hellweg, 2004]. This may illustrate the difference in anelastic attenuation for the two wave types, or may be related to the f_{max} observed by Hanks [1982].

For large events, stressdrop is often calculated independently using aftershock area as an alternate estimate of the rupture area [for a review, see Das and Henry, 2003], and surface rupture or deformation measurements to give an estimate of slip. By estimating slip for small, repeating events in the Parkfield segment of the San Andreas Fault from the tectonic rate, Nadeau and Johnson [1998] found their stress drops to be dependent on moment. For small events, such independent observations of rupture area and/or slip are rare. Although most of the events were recorded only at a single station, we can use the polarization of P- and S-waves along with t_{S-P} to map their locations [Abercrombie, 1995a]. For the nearby 1977 Briones sequence, Bolt et al [1977] found the M_L 4.2 mainshock to be bracketed by fore- and aftershocks which occurred above and below. It is likely that a map of the MS and MAS aftershocks will define the limits of their rupture areas. The strainmeter steps associated with them can give an estimate of slip. For these two events, we can then calculate independent stressdrop estimates.

From the catalog of triggers from the borehole geophone at BRIB, it is clear that the foreshock and each of the larger aftershocks has its own aftershock sequence. Hundreds of small events of the sequence were recorded by the borehole geophone (Figure 3). As part of the event mapping process, we will refine this catalog of triggers and, when possible, locate the aftershocks using polarization and t_{S-P}. We will use
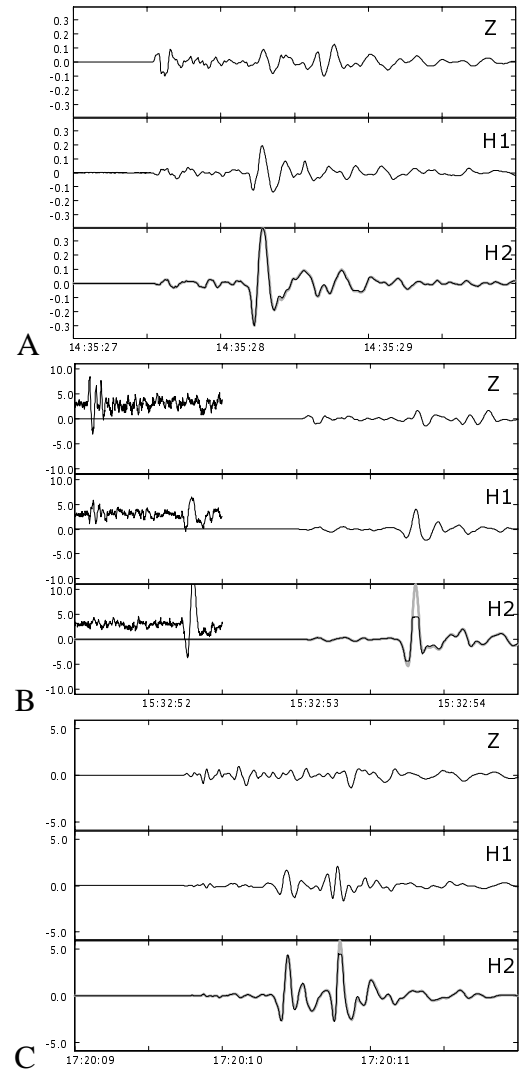

Figure 2: Unfiltered three-component seismograms for the (A) M_d 2.5 foreshock (FS), the (B) M_L 3.5 mainshock (MS) and the (C) M_L 3.4 aftershock (MAS). In each case, H2 is represented by the geophone trace (black) and the integrated and instrument corrected accelerometer trace (gray). (A) Note the good agreement between the accelerometer and velocity traces for H2. (B) The trace before the MS is multiplied by 100,000 to show a small event (approximately M_L=-1.5). (C) The MAS is two or more events separated by about 0.4 s. Amplitude is shown in mm/s and time is given in UTC on 19 Oct 2003 (A, B) and 20 Oct 2003 (C).
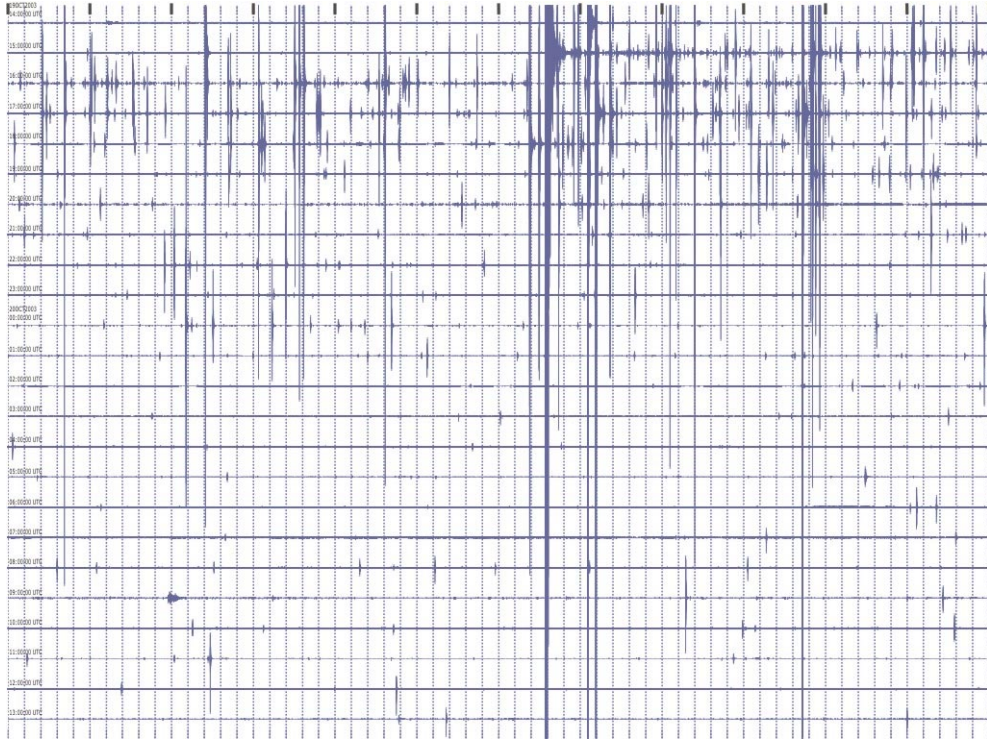
Figure 3: Helicorder-like record for the first 24 hours of the Orinda sequence. The record starts at 19 Oct 2003, 14:00 UTC, 35 minutes before the FS. Each trace is 1 hour, and the traces are exaggerated vertically, so that the FS and MS are clipped, but many tiny events can be seen.

these locations to map rupture areas for events in the sequence with magnitudes greater than 1. If this is possible, we will have independent area estimates for these events for use in the calculation of stressdrops.

The question of the scaling-invariance of earthquakes is only one of the questions about the physics of earthquake rupture which remain open. For large earthquakes, fore- and particularly aftershocks are often studied thoroughly to give answers about the relationship between development of stress and strain in the nearfield [i.e. Das and Henry, 2003]. Myriad aftershocks down to magnitude –2.5 are rarely measured in tectonic settings, as the mainshocks are usually too far from the nearest seismometer and large events often saturate the record. For the Orinda sequence, a simple bar graph of the number of triggers as a function of interval demonstrates that each big event, starting with the M_d 2.5 FS has its own
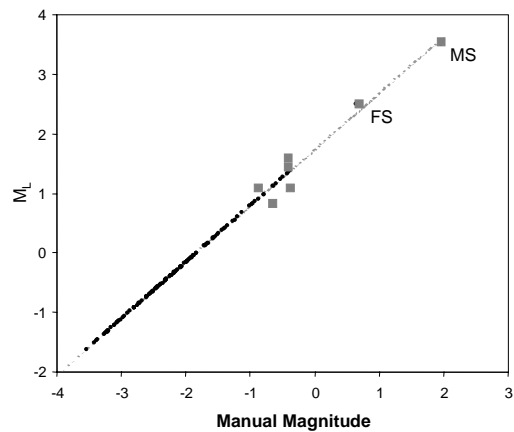

Figure 4: Calibration of manual magnitude to M_L/M_d for more than 100 events of the Orinda sequence using 7 events from the NCSN catalog (gray squares). The best fit line used to convert from M_{man} to M_L is: $M_L = 0.95\ M_{man} + 1.73$. The black dots show the range of ML for about 100 events of the Orinda sequence.

aftershocks. As an integral part of the data analysis, we can look at the dynamics and statistics of this foreshock-mainshock-aftershock sequence. What is the smallest earthquake for which we can describe an aftershock sequence? How do the locations of the aftershocks develop over time? Does the b-value change during the sequence? Is it the same for the aftershocks?

There is clearly rupture complexity in the MAS (Figure 2C), and it is also apparent in many of the smaller events [Hellweg, 2005b]. Are such pulses actually separate events which happen to
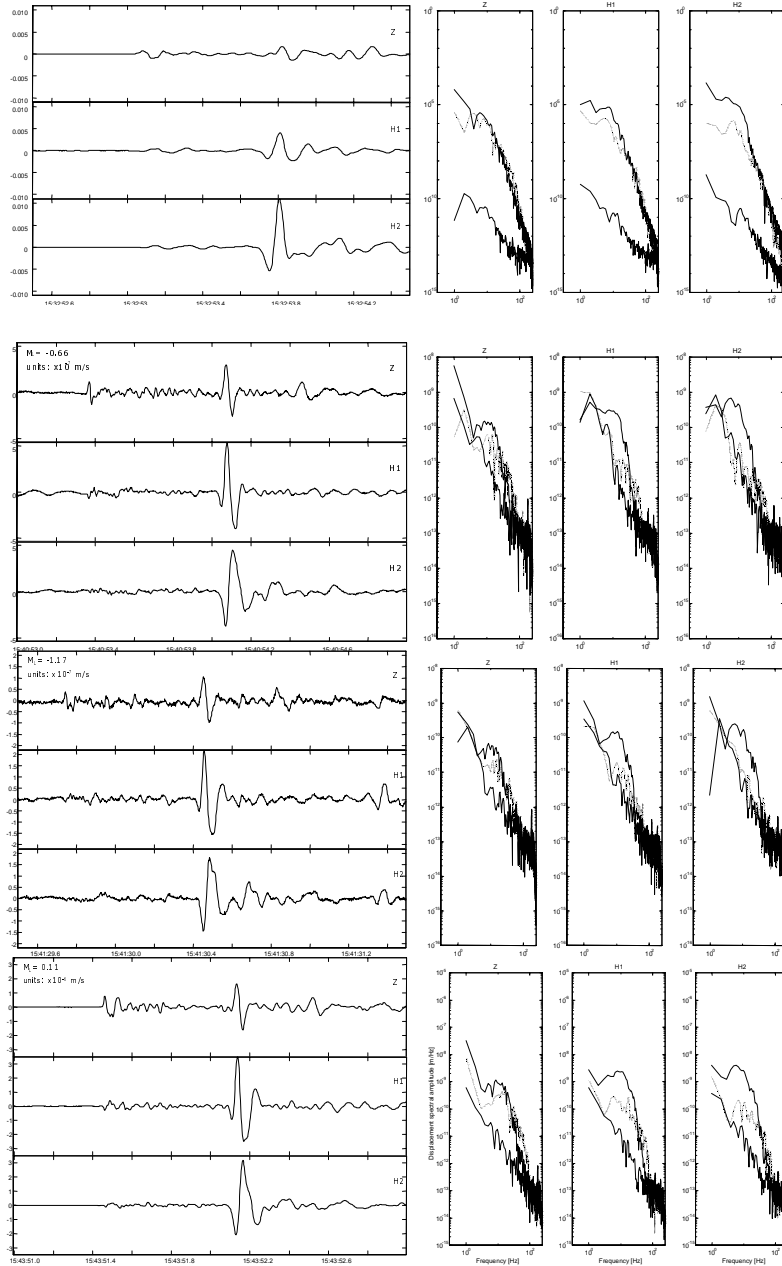

Figure 5: Three-component, instrument-corrected (IC), velocity seismograms for the MS and 7 small aftershocks, and IC displacement spectra of 0.5 s P, S and pre-event noise intervals. Seismogram units are m/s, with the exponent given in the upper left hand corner along with M_L for each event. Spectra show frequency from 1 to 200 Hz (horizontal axis) and spectral amplitude in m/Hz.

occur at almost the same time, are the later events triggered, or are the pulses due to propagating rupture? Mapping of the subevent locations [Plesinger et al, 1986, Abercrombie, 1995b] and
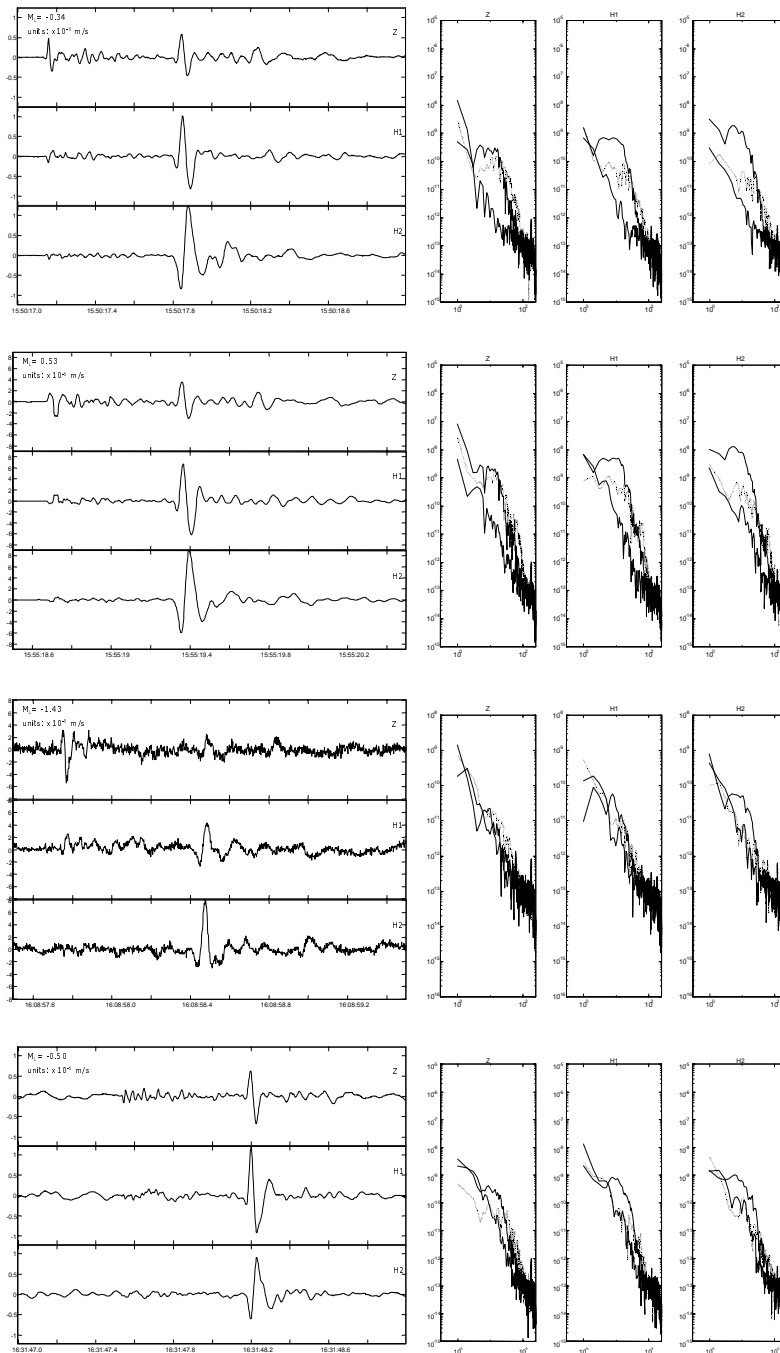

Figure 5 (cont)

emprical Greens function analysis [Mori and Hartzell, 1990, Dreger, 1994, Fletcher and Spudich, 1998, Hellweg and Boatwright, 1999] will offer insights.

The Orinda sequence occurred in a part of the San Andreas Fault System in the San Francisco Bay Area with very little seismicity. A previous swarm in 1977 [Bolt et al, 1977], was located 3 km to the WSW of the Orinda mainshock at a depth of 9.5 km. The fault plane solution for the 1977 mainshock is clearly similar to the moment tensor for the MS and MAS (Figure 1), which

occurred at a depth of about 5 km or shallower. Bolt et al [1977] mapped the 1977 event, as well as a number of fore- and aftershocks onto a plane dipping SW. They projected the plane to the ENE, where it intersected the surface near Concord, California. The ruptures of the 2003 sequence may have occurred at a shallower depth on the same fault. However, the mechanisms are also consistent consistent with the motion observed by Unruh and Kelson [2002] on the Lafayette and Reliez Valley faults which lie between the Hayward and Calaveras Faults. In addition to providing input into the evaluation of the scaling controversy and an investigation of aftershock location and statistics, mapping the faults on which the Orinda and other sequences occurred will support the evaluation of earthquake hazards in this populated area.

Besides its serendipitous location, almost directly under BRIB, the Orinda sequence was the first to occur after the initiation of continuous, high sample rate recording of the borehole geophone. In the three years since, several other seismic sequences exhibiting similar characteristics have occurred nearby (Figure 1). Most recently a sequence starting on 18 Feb 2006 and located 13.7 km SSE of BRIB near Moraga, has two large events (M_L 3.2 and M_w 3.7), and on-going aftershocks. As they also are tight clusters of events, we will investigate them using the same methods we have applied to the Orinda sequence. The addition of these more distant events will allow an investigation into the affects of attenuation and/or f_{max} on the high frequency energy present in the tiny earthquakes, and their implications on assessing source scaling.

The principle **intellectual merit** of this proposal lies its contribution to the our understanding of the physics of small earthquakes. The beauty of the Orinda sequence as a tool for investigating the physics of earthquake processes stems from its location nearly below the borehole at the station BRIB in an otherwise seismically quiet area. The other event sequences will provide further support in that we can assess the effects of attenuation and f_{max} on the recordings of tiny events as their distance from the station increases. We have onscale recordings over more than 5 units of magnitude for thousands of events located in what for seismic purposes are tight clusters, perhaps one cubic kilometer in volume. Waveforms, even for large and small complex events, are very simple. And, as there is no nearby seismicity, we can discriminate between events of these sequences and other earthquakes on the basis of t_{S-P} and polarization. One of the **broader societal impacts** of the study follows from the mapping of the hypocenters of the earthquakes of the Orinda and other nearby sequences as part of the investigation of scaling. It will help to characterize faults of the San Andreas fault system in the San Francisco Bay Area which have very low seismicity and about which relatively little is known otherwise [Unruh and Kelson, 2002, Parsons et al, 2003]. Thus, it will support the estimation of earthquake hazards in this populated area. As these earthquakes occurred in a well-populated area, they generate excitement and interest locally. We will incorporate information about the Orinda and other nearby sequences and what we have learned from it in BSL's outreach activities, with presentations as part of the annual open house and the tours for groups from local schools and other organizations. A second **broader societal impact** lies in that the data and their analysis form a unique teaching tool. It is vitally important that students of seismology and geophysics acquire an understanding the pitfalls associated with the processing and analysis of waveform data. Examples of methods and analysis of the Orinda sequence will be incorporated as hands-on discovery exercises on waveform analysis and earthquake scaling in several classes.

3.   PROJECT PLAN

Overview of the Problem

For the earthquakes in the Orinda sequence as recorded at BRIB, the differences in the effects of both path and site are negligible. The mainshock is small, so the aftershocks presumably populate a very small volume. For 96 events, we have measured t_{S-P} which lies between 0.58 s and 0.72 s. Taking average P and S velocities for the near surface layers in the velocity model *gil7* [Romanowicz and Dreger, 1994], 4100 and 2300 m/s, respectively, the hypocentral distances of the events from the station lie between 3.1 and 3.7 km. For a selection of events, azimuth and incidence angles range from 83° - 121° and from 2° - 30°, respectively. We propose to explore the scaling of moment, energy and stressdrop over a range of event sizes, $M_L \sim$ -1.5 to 3.5 [Hellweg, 2004, 2005a, 2005b, 2006], using measurements from P- as well as S-waves in both the time and frequency domains. Using codes adapted from Abercrombie [1995b], we will study and evaluate spectra from P- and S-waves recorded

Figure 6: Three dimensional locations of FS (black), MS (red) and several aftershocks (gray) of the Orinda sequency. The station is indicated by the inverted triangle at the surface. Hypocentral distances were calculated using t_{S-P} for each event and v_P=4.1 km/s, v_S=2.3 km/s. The direction from the station was inferred from the azimuth and incidence angles measured from the P wave.

by all three components of the BRIB geophone. In addition, we will calculate moments from time domain measurements of the P- and S-pulses [Seidl and Hellweg, 1988, Uhrhammer, 1993], as well as from single station moment tensor inversions [Uhrhammer, 1993]. For small events, stressdrop is generally calculated using the moment and an estimate of the dimensions of the source calculated from the corner frequency. The interpretation of the corner frequency into an event area is dependent on the model. We propose to map the areas of the large events of the sequences using aftershock locations. Although most of the events were only recorded at a single station, we can use the polarization of P- and S-waves along with t_{S-P} to map their locations relative to the station (Figure 6) [i.e. Abercrombie, 1995a, Plesinger et al, 1986]. We will use this map to determine rupture areas of the two largest events, the MS and MAS, which we will then compare with the estimates of the source dimension from the spectral and time domain measurements. It is clear from the catalog of triggers from the borehole geophone at BRIB that the foreshock and each of the larger aftershocks has its own aftershock sequence. While we will investigate the statistics of these sequences, we will use also use their locations to map rupture areas for some of the larger aftershocks. For each event with an independent estimate of area, we will calculate the stressdrop and compare it with the estimate from the moment and corner frequency. We will also refine the catalog and use it to investigate the differences between the
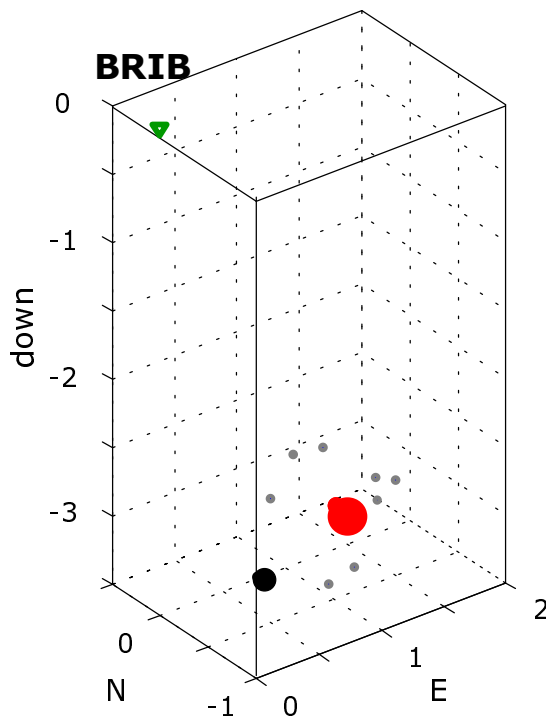
mainshock, the foreshocks and the aftershock. Can each large aftershock be considered a mainshock? What is the smallest earthquake which has an aftershock sequence? Can we map these sequences to determine a rupture area for each? If so, their areas will be used in stressdrop calculations. In addition, we will look at the sequence of aftershock locations to investigate how they trigger each other. In the waveforms of individual events of many different sizes, rupture complexity apparent (Figure 2, 5). As we look at and analyze the waveforms, we will examine them for nucleation phases [Beroza and Ellsworth, 1995, Ellsworth and Beroza, 1998], and we will attempt to model their rupture processes using empirical Greens functions [Dreger, 1994, Hellweg and Boatwright, 1999] and compare the results to the mapped aftershock seismicity.

In this project, mapping the hypocenters will contribute to understanding the rupture process occurring in these small earthquakes. It will provide an additional bonus in terms of hazard assessment in the hills of San Francisco's East Bay. In this region, the topography is complex, mapped seismicity is rare, and the faults are relatively unknown [Unruh and Kelson, 2002, Parsons et al, 2003].

Preliminary Results

Since the beginning of the Northern California Seismic Network (NCSN), very little seismicity has been recorded just to the north-east of Orinda, California. Prior to the 2003 sequence, only a single cluster of earthquakes occurred 3 km WSW of the Orinda sequence in January, 1977 [Bolt et al, 1977]. The 2003 sequence began on 19 Oct 2003 at 14:35:27 UTC with a M_d 2.5 FS. During the week before the foreshock, none of the triggers from the borehole geophone at BRIB were associated with events with $t_{S-P} < 1$ s. The closest events were a number of small quakes with $t_{S-P} \sim 2.2$ s, associated with seismicity near Danville, CA, on the Calaveras fault (Figure 1). Both the M_L 3.5 MS of the 2003 Orinda sequence, on October 19, and the M_L 3.4 MAS the following day clipped on the E component of the surface velocity sensor (Guralp CMG-3T) at BRIB and on one of the two horizontal components of the 3-component borehole geophone (Oyo HS-1) geophone. Fortunately, the clipped component of the geophone corresponds to the working component of the borehole accelerometer (Wilcoxon 731A). To demonstrate that the accelerometer component H2 can be used in place of the corresponding velocity component, we plot three component geophone recordings of the FS, MS and MAS in black in Figure 2. For these plots, the accelerometer trace, shown in gray, has the instrument response removed and has been integrated to velocity. The similarity in the H2 components for the FS is better than 1%, indicating that the integrated H2-accelerometer record can be use in place of the clipped geophone record for the MS and MAS. In addition to the seismometer and accelerometer recordings, both the MS and the MAS caused steps on the strainmeter record.

To get an idea of the range in sizes of the events, we have calibrated a manual magnitude scale for the Orinda sequence, based on Richter's original method [Richter, 1935, Hellweg 2004, 2005a, 2006]. About 15 of the events in the sequence were located by the Northern California Seismic Network (NCSN) and their magnitudes determined, M_L for the two largest (MS, MAS), M_d for the others. For seven of the events listed in the catalog which occurred in the first few hours of the sequence, we calculated manual magnitudes, which we used to calibrate the manual magnitude to the M_L/M_d scale (Figure 4) [Hellweg, 2004, 2005a, 2006]. The best fit line to these events gives $M_L = 0.95 M_{man} + 1.73$. We then determined manual magnitudes for more than 90 small events of various amplitudes and calculated the corresponding M_L/M_d value. The smallest events for which we determined manual magnitudes correspond to $M_L \sim -1.5$.

The sequence includes the FS, the MS and a MAS as well as more than 4000 aftershocks ranging in magnitude from –1.5 to 2.7 over the course of the next 3 months. Figure 3 shows a helicorder-like record for the first 24 hours of the sequence. Each of the small or large spikes is one of the numerous events belonging to the sequence. Figure 5 shows instrument-corrected velocity waveforms and instrument-corrected displacement spectra from the P and S waves, and from a 0.5 s window of noise before the P wave onset for eight events with a variety of magnitudes. It demonstrates that both the waveforms and spectra for a range of event sizes can be analyzed. We have also used polarization analysis [Plesinger et al, 1986, Abercrombie, 1995 a] to "locate" a small subset of events (Figure 6). The aftershocks analyzed clearly map to a circle surrounding the MS location.

 Summary of the proposed study

The major, interwoven components of the project address open questions about small earthquakes: their scaling, complexity of rupture, and the statistics and physics of fore-, main- and aftershocks. For this, a catalog of the events in each sequence must be developed, based on the time-domain analysis of the waveforms. The catalog will include an identifing time and size for each event. It will also include other information, such as the event's distance from the station in the form of t_{S-P}, its direction from the geophone (azimuth and incidence angle of the P-wave) and the periods and amplitudes of the P and S phases. Taking off from the trigger catalog at BRIB, we will use visual inspection and interactive analysis to determine these parameters, as well as characterizing each event as "simple" or "complex". "Complex" events will have several P wave pulses before the S wave onset or will be a member of a rapid sequence of events. Because of the amount of data, only the 500 sps data from the vertical component of the borehole geophone has been recorded continuously. Data for the two horizontal components is only stored occasionally, in association with a trigger. For the first several days of the Orinda sequence, however, many continuous hours of three-component data have been archived. Nonetheless, these few hours of three-component data include more than several hundred earthquakes over a large range of sizes. From the events in the intervals in which three-component data is available, we will determine which parameters characterizing an event can be measured robustly from only the vertical component. Because we have three-component data for so many events of different sizes, we can compare measurements from the Z-component with those from the horizontal components. We will be able to develop a means of projecting measurements from a single (Z) component to the three-component estimates of spectral amplitudes, corner frequency, and pulse area, period and amplitude. For larger events of the sequences, we will use data from NCSN stations as well as other stations of the BDSN and NHFN for locations and characterization.

The measurements for most scaling studies are made in the frequency domain [i.e., Abercrombie, 1995b, Prieto et al, 2004]. We have the Matlab codes used by Abercrombie [1995b] for frequency domain measurements of the low frequency level and of the spectrum, and will adapt them to this dataset. Figure 5 shows velocity seismograms from eight Orinda events ranging in magnitude from M_L –1.43 to 3.5, as well as instrument-corrected displacement spectra for 0.5 s data windows (250 samples) from all three geophone components for the P- and S- waves and from a pre-event noise interval. For the smallest event shown, the P- and S-waves are clearly visible in the vertical and horizontal seismograms, respectively. The spectra show the relationship of signal and noise (S/N) as a function of frequency. While S/N issues exclude the

very smallest events from analysis, slightly larger events may be analysed. As there are many tiny events, it may be possible to apply summation techniques [i.e. Prieto et al, 2004] to improve the S/N ratio, so that analysis can be extended to even smaller magnitudes. When the S/N ratio allows it, we will also measure the area under the P- and S- pulses in the displacement waveforms as well as their period to make time-domain determinations of moment and source dimension [Seidl and Hellweg, 1988, Uhrhammer, 1993]. We will use the measurements from both the time- and frequency domains to explore the scaling of moment, energy and stress drop over the entire range of event sizes. Moment tensors have been determined for the MS and MAS of the Orinda sequence and for the largest event of the Moraga sequence (Figure 1). In the determination of the moment, it will be important to correct for the mechanism properly, rather than using an average value for the radiation pattern. We will use a single station moment tensor method [Uhrhammer, 1993] to determine moments and mechanisms for small events when possible.

As we evaluate the waveforms for event moment and dimension, we will use t_{S-P} and waveform polarization to locate events for which three-component data exist, relative to BRIB [Abercrombie, 1995a]. In a set of events ranging in magnitude from -.2 to 2.5, we determined azimuth and incidence angle from displacement hodograms of the P-wave. Azimuths range from 83° to 121° and incidence angles range from 2° to 30° (Figure 6). The interpretation of these angles to determine event location depends on the velocity structure, which we must investigate more carefully. We will do this by reviewing and revising the location determinations for the events which made it into the NCSN catalog as well as other small events from the sequences for which we have been able to find usable waveforms in the NCSN, BDSN and NHFN datasets, at the same time improving the velocity model for the region around the hypocenters and the station BRIB. We will further constrain the velocity model by modeling the three-component waveforms for the MS and MAS. The locations of the events will give a map of the fault, perhaps an extension of that defined by Bolt et al [1977] or by Unruh and Kelson [2002]. In addition, the event locations can provide an estimate of the rupture area. Given the large number of small earthquakes, however, it may be that we can determine rupture areas for the FS and for several of the large aftershocks as well as for the MS and MAS. We will incorporate these independent estimates of rupture area into the stress drop analysis. Event and sub-event locations determined using polarization analysis [Hellweg, 2005b] will prove important in the analysis of event complexity as well.

Tasks

The success of this project depends on the creation of an event catalog from the BRIB recordings of the sequences and careful measurements of many parameters from the waveforms and their spectra. These measurements are fundamental to investigating scaling for the small earthquakes, as well as the investigations of event complexity and nucleation phases. They will also be important input into determining the effects of attenuation and/or f_{max} on the observations. Part of the early work will be to create procedures for making measurements which are reliable for both tiny events, when the signal-to-noise ratio may be poor, and the larger events of the sequences. As we make the measurements, it will also be important to explore the limits of the methods for small events and their application to events recorded only with the vertical geophone.

The trigger list for the Orinda sequence at BRIB includes more than 4000 events over more than 3 months following the MS, most of which occurred during the first 48 hours. We have made a cursory examination of several hours of data and looked more closely at more than 90 events of various sizes. Many of the events can be recognized as events but will not be susceptible to analysis as their S/N ratio will be too low (Figure 5, M_L –1.43). Other events, like the MAS (Figure 2C), may be excluded from scaling analysis because they are doublets or multiplets in the sense that additional P-waves arrive between the P- and S-waves of an event, or possibly the rupture of these events procedes in bursts. Nonetheless, we will perform careful measurements on these events, as well, so that we can investigate the cause of their complexity. We estimate that we will be able to perform scaling analysis for more than 10 percent of the events associated with the triggers, providing a large number of measurements across a broad range of event sizes. Similar numbers of observations will result from the analysis of the later sequences.

Year 1
1) Develop an event catalog based on the BRIB trigger list. The trigger list for the BRIB borehole geophone will be the basis for a catalog of the events of the Orinda and later sequences. Due to the high sample rate (500 sps) and sensitivity, even very tiny events with high frequency content are visible in the recordings. We will develop a refined catalog using cross-correlation and evaluate each event, determining *(a)* onset time, *(b)* manual magnitude [Hellweg, 2004, 2005a, 2006], time-domain estimates of *(c)* P-pulse period (Z component) and amplitude (Z, H1, H2 components), *(d)* S-pulse period (usually H1 component) and amplitude (Z, H1, H2, or Z, N, E), *(e)* radiated energy, frequency domain estimates of *(f)* low-frequency spectral level and *(g)* corner frequency for both P- and S-waves, as well as *(h)* t_{S-P}, *(i)* azimuth, and *(j)* incidence angle for determining the location. For complex events, a similar set of measurements will be performed, with a suite of values measured for each P-arrival. Spectral measurements will not be calculated for these events, as the spectral windows will be too short. For the subset of events for which waveforms were recorded at other stations of the BDSN, the NCSN and the NHFN, we will incorporate measurements from those waveforms as well. For the large number of small events in these sequences, this will take some time.
2) Locations, as well as moment and energy estimates depend on the model of the medium we use in the interpretation. The currently existing velocity model for the region around the hypocenters and the station BRIB is very coarse. Intially, we will review and revise the locations of the events which are listed in the NCSN catalog, at the same time improving the velocity model particularly in the region encompassing the hypocenters and BRIB. We will then perform waveform modeling for at least the two largest events, the MS and MAS, based on their moment tensor mechanisms and their redetermined hypocentral locations. The modeling will include the far-field P and S waves as well as the intermediate steps registered on the strainmeter. In addition to the timing of the phases the modeling will fit the observed angle of incidence of the P wave. We will apply the same modelling to the events of the other sequences. The constrained velocity model will then be used to map the locations of the other events as described below.
3) Map the locations of events using t_{S-P}, azimuth and incidence angle to determine *(a)* the position of the sequence with respect to the faults mapped by Bolt et al [1977] and by Unruh

and Kelson [2002], and *(b)* rupture areas for the largest quakes of the sequence [Das and Henry, 2003].

Year 2
1) Determine relative moments and moment tensors for the smaller earthquakes of the sequences recorded only at BRIB using the single station method of Uhrhammer [1993]. We will investigate how the moment tensors of small events relate in time and space to that of the MS and to the "large" aftershock immediately preceding them.
2) Use the measurements tabulated in the catalog to assess the physics of rupture, comparing time- and frequency-domain estimations of moment, energy and stress drop for events of different sizes. Does the apparent stress drop depend on moment? How do the moments and stressdrop estimates based on the frequency domain measurements compare with those based on the "independent" measure of event area using aftershock mapping? How does anelastic attenuation affect the results? Is f_{max} an issue [Hanks, 1982]? Do measurements from the time- and frequency domain give different results?
3) From the catalog and event mappings, we will investigate the statistics and physics of the aftershock sequences: what is their timing; can we discriminate between the events belonging to one large event of a sequence an another; does the b-value change as the sequences develop?

With waveform data for 4000 events, the catalog will take some time to complete. Dr. Hellweg and the graduate student will share this work, as well as in the waveform modeling of the large events to improve the velocity structure. They will develop and adapt a cross-correlation code to select the events, but review each event "manually". This is particularly important for the smallest events, where the signal-to-noise ratio is poor. Based on the waveform analysis, as many events as possible across a broad range of sizes, will be selected for the scaling and event location studies. The frequency-domain analysis will be based on the MatLab codes developed by Abercrombie [1995b].